NEOPLASIA
www.neoplasia.com
Volume 14 Number 2 February 2012 pp. 84–94 84

Merlin/NF2 Regulates Angiogenesis in Schwannomas through a Rac1/Semaphorin 3F–Dependent Mechanism[1]

Hon-Kit Wong[*,2], Akio Shimizu[†], Nathaniel D. Kirkpatrick[*], Igor Garkavtsev[*], Annie W. Chan[‡], Emmanuelle di Tomaso[*,3], Michael Klagsbrun[†] and Rakesh K. Jain[*]

*The Steele Lab of Tumor Biology, Department of Radiation Oncology, Massachusetts General Hospital and Harvard Medical School, Boston, MA, USA; [†]Departments of Surgery and Pathology, Children's Hospital Boston and Harvard Medical School, Boston, MA, USA; [‡]Department of Radiation Oncology, Massachusetts General Hospital and Harvard Medical School, Boston, MA, USA

Abstract

Neurofibromatosis type 2 (NF2) is an autosomal-dominant multiple neoplasia syndrome that results from mutations in the NF2 tumor suppressor gene. Patients with NF2 develop hallmark schwannomas that require surgery or radiation, both of which have significant adverse effects. Recent studies have indicated that the tumor microenvironment—in particular, tumor blood vessels—of schwannomas may be an important therapeutic target. Furthermore, although much has been done to understand how merlin, the NF2 gene product, functions as a tumor suppressor gene in schwannoma cells, the functional role of merlin in the tumor microenvironment and the mechanism(s) by which merlin regulates angiogenesis to support schwannoma growth is largely unexplored. Here we report that the expression of semaphorin 3F (SEMA3F) was specifically downregulated in schwannoma cells lacking merlin/NF2. When we reintroduced SEMA3F in schwannoma cells, we observed normalized tumor blood vessels, reduced tumor burden, and extended survival in nude mice bearing merlin-deficient brain tumors. Next, using chemical inhibitors and gene knockdown with RNA interference, we found that merlin regulated expression of SEMA3F through Rho GTPase family member Rac1. This study shows that, in addition to the tumor-suppressing activity of merlin, it also functions to maintain physiological angiogenesis in the nervous system by regulating antiangiogenic factors such as SEMA3F. Restoring the relative balance of proangiogenic and antiangiogenic factors, such as increases in SEMA3F, in schwannoma microenvironment may represent a novel strategy to alleviate the clinical symptoms of NF2-related schwannomas.

Neoplasia (2012) 14, 84–94

Abbreviations: HMVECs, human microvascular endothelial cells; HUVECs, human umbilical vascular endothelial cells; NF2, neurofibromatosis type 2; NRP, neuropilin; ROCK, Rho-associated coiled-coil forming protein serine/threonine kinase; SEMA, semaphorin; TSP2, thrombospondin 2; VEGF, vascular endothelial growth factor

Address all correspondence to: Rakesh K. Jain, PhD, Harvard Medical School and Edwin L. Steele Laboratory for Tumor Biology, Department of Radiation Oncology, Massachusetts General Hospital, 100 Blossom St, Cox 7, Boston, MA 02114. E-mail: jain@steele.mgh.harvard.edu

[1]This work was supported in parts by grants from the National Institutes of Health (P01-CA80124 to R.K.J. and CA37392 and CA45548 to M.K.), Federal Share/National Cancer Institute Proton Beam Program Income Grant (to R.K.J.), the Claflin Award (to E.d.T.), and the Flight Attendant Medical Research Institute (A.W.C.). The authors have no conflicts of interest to declare.

[2]Present address: Center for Neurologic Diseases, Brigham and Women's Hospital and Harvard Medical School, Harvard Institutes of Medicine, Boston, MA 02115.
[3]Present address: Novartis Institute of Biomedical Research, Cambridge, MA 02139.

Received 16 November 2011; Revised 3 February 2012; Accepted 3 February 2012

DOI 10.1593/neo.111600

Introduction

Neurofibromatosis type 2 (NF2) is an autosomal-dominant multiple neoplasia syndrome that results from mutations in the NF2 tumor suppressor gene located on chromosome 22q. Patients mainly develop nervous system tumors (schwannomas and meningiomas), peripheral neuropathy (damage to nerves of the peripheral nervous system), and eye and skin lesions to a lesser extent [1]. Although most patients with sporadic schwannomas benefit from surgery, patients with NF2 have limited options owing to the multiplicity and bilateral location of their tumors [2]. The hallmark feature of NF2, vestibular schwannomas, is particularly challenging surgically because of the potential for brainstem or cranial nerve damage—hearing loss and tinnitus are very common in these patients.

Our group recently provided encouraging clinical evidence that bevacizumab, an anti–vascular endothelial growth factor (VEGF) antibody treatment, improved hearing and stabilization of tumor growth in patients with bilateral vestibular schwannoma [3] and subsequently delineated the mechanisms by which anti-VEGF treatment might have produced such clinical outcomes [4]. Keeping in line with the published data that VEGF is expressed in schwannomas [5–8], our preclinical and clinical results clearly show that VEGF and tumor angiogenesis are essential determinants in schwannoma progression and its associated clinical symptoms. More importantly, during the course of analysis, we discovered that the expression of class 3 semaphorins (SEMA3), particularly SEMA3A and SEMA3F, was markedly decreased in NF2-related schwannomas, whereas that of VEGF remains unchanged. This observation led to a hypothesis that the relative balance of VEGF and SEMA3 expression regulates physiological angiogenesis in normal nerve tissues. With reduced levels of functional wild-type merlin/NF2 in schwannomas, the ratio of VEGF levels to SEMA3s increases and contributes to abnormal angiogenesis, tumor growth, and progression [9]. However, a causal link between merlin/NF2 and SEMA3s as well as the role of SEMAs in pathologic schwannoma angiogenesis remains not established.

SEMA3s are secreted proteins that were first shown to regulate axon guidance in the developing nervous system [10–13] and subsequently found to also regulate both physiological and pathologic angiogenesis [14–17]. In general, SEMA3s first bind to neuropilin (NRP) and plexins to transduce intracellular signals and exert their antiangiogenic functions [18]. Specifically, SEMA3F, in an NRP2-dependent manner, can inhibit cell adhesion and cell migration *in vitro* and tumor angiogenesis and metastasis *in vivo* [19,20]. Furthermore, it has been recently shown that ABL2 and RhoA play key roles in mediating SEMA3F-induced depolymerization of F-actin and the subsequent cytoskeleton collapse in tumor cells and endothelial cells [21].

In this study, we report that merlin/NF2 upregulates SEMA3F expression through Rho GTPase Rac1. Furthermore, we show that SEMA3F is indeed an essential molecule to regulate angiogenesis and normalize vessels in orthotopic preclinical tumor models of NF2 through reduction in vessel density and increased pericyte vascular coverage. Taken together, our results suggest that the mutation in NF2 directly contributes to tumor angiogenesis through modulation of SEMA3F expression. Interestingly, merlin/NF2 also induced the expression of other antiangiogenic factors such as thrombospondin 2 (TSP2) whose precise role in NF2-mediated angiogenesis needs to be investigated.

Materials and Methods

Chemical Reagents and Antibodies

Recombinant C3 transferase (CT03) was purchased from Cytoskeleton (Denver, CO). Y-27632 (688001) and Rac1 (553502) inhibitor were purchased from Calbiochem (Darmstadt, Germany), and Evans Blue dye was purchased from Fisher Scientific (Waltham, MA). Lentiviral particles expressing merlin short hairpin RNA (shRNA; L271) and scramble (Lmag) were kind gifts from Dr Marianne F. James (Centre for Human Genetic Research, Massachusetts General Hospital, Richard B. Simches Research Building). The following antibodies were used in notated dilutions: β-tubulin (1:10,000, MAB3408; Chemicon, Billerica, MA), merlin (1:1000, sc-331/A-19; Santa Cruz Biotechnology, Santa Cruz, CA), Rac1 (1:1000, ARC03; Cytoskeleton), semaphorin 3F (SEMA3F, 1:3000; GenScript, Piscataway, NJ), TSP2 (1:2000, 611150; BD Transduction Laboratories, Sparks, MD), and V5 (1:5000, 46-0705; Invitrogen, Grand Island, NY).

Constructs

The pMOWSdSV-dsred retroviral construct was a kind gift from Prof Brian Seed (Department of Genetics, Massachusetts General Hospital and Harvard Medical School) [22]. Murine SEMA3F or TSP2 was cloned into pMOWSdSV using *Pac*I and *Sal*I sites. Murine SEMA3F (in pCMV-SPORT6, MMM1013-65024) and TSP2 (in pcDNA3, plasmid 12411) was obtained from Open Biosystems (Rockford, IL) and Addgene (Cambridge, MA), respectively. SEMA3F was amplified from pCMV-SPORT6 using forward 5′-GCGCTTAATTAAACC ATGGTTGTCACTGCCTTCATC and reverse 5′-GCGCGTCGACT-CACGTAGAATCGAGACCGAGGAGAGGGTTAGGGATAGGCT-TACCTGTGTCCGGAGGGTGGTGGCG primers. TSP2 was amplified from pcDNA3 using forward 5′-GCGCTTAATTAAAC-CATGGTCTGGGCACTGGCCCTG and reverse 5′-GCGCGTC GACTCACGTAGAATCGAGACCGAGGAGAGGGTTAGGGA-TAGGCTTACCGGCATCTCT GCACTCATACTT. All the cloning-related polymerase chain reaction (PCR) amplifications were done with PfuUltra DNA polymerase (Agilent Technologies, Santa Clara, CA) using a standard protocol. Sequencing was performed by MGH DNA Core Facility (Boston, MA).

Generation of Rac1 shRNA Retroviruses

ShRNA against mouse Rac1 (5′-GCATTTCCTGGAGAGTA-CA-3′ [23]) was cloned into pSilencer 5.1-U6 construct (AM5782) according to the standard instructions (Ambion, Grand Island, NY), with pSilencer 5.1-U6 Retro scrambled (5783G) as a control. pSilencer 5.1_U6_Rac1shRNA was then cotransfected with GAG/POL and VSV plasmids into HEK293T cells to produce retroviruses (see next section for the transfection procedures).

Cell Lines and Generation of Stable Cell Lines

The original clone of human HEI193 [24,25], which contained a mutated copy of merlin/NF2, was a gift from Dr Xandra Breakefield. Subsequent analysis of our HEI193 revealed that our clone did not contain a wild-type copy of merlin/NF2 [4]. The generation of murine *Nf2*−/− tumor Schwann cells has been described previously [4], and these cells were kindly provided by Drs Andrea I. McClatchey and Annie Chan. We verified that the *Nf2*−/− cells were merlin deficient through Western blot analysis. Both cell lines were kept in Schwann cell medium supplemented with Schwann cell supplement, 5% fetal bovine serum, and penicillin/streptomycin (ScienCell 1701, Carlsbad, CA). Human umbilical vein endothelial cells (HUVECs) were maintained in endothelial growth medium (EGM) supplemented with bovine brain extract (CC-3024A; Lonza, Basel, Switzerland), human microvascular endothelial cells (HMVECs) were maintained in 1× EBM-2 (CC-3156; Lonza) supplemented with EGM-2 MV (CC-4147; Lonza),

and U87MG was maintained in 1× Dulbecco modified Eagle medium (10-014-CV; CellGrow, Manassas, VA) supplemented with 10% fetal bovine serum. To generate *Nf2*−/− cell lines overexpressing SEMA3F or TSP2, pMOWSdSV-SEMA3F or pMOWSdSV-TSP2 was transfected into HEK293T cells with GAG/POL and VSV in a 3.3:2.3:1 ratio using Lipofectamine 2000 (Invitrogen). Culture medium containing retroviruses was collected 1 and 2 days after transfection. *Nf2*−/− cells were infected with SEMA3F or TSP2 retroviruses multiple times to ensure virtually 100% expression levels.

Tube Formation Assay

The effect of conditioned medium from various genetically modified *Nf2*−/− cells on the endothelial cell structures and morphologies was investigated with endothelial cell tubes formed with HUVECs. Growth factor–reduced Matrigel (354230; BD Biosciences, Sparks, MD) was first plated in a 24-well plate and allowed to solidify for 30 minutes at 37°C with 5% CO_2. One hundred thousand cells were then seeded on top, and tubes were allowed to form for 2 hours. Conditioned medium was added, and the effect on tube structure and morphology was examined with bright-field microscopy for 36 hours.

Animal Models

To recapitulate as closely as possible the microenvironment of vestibular schwannomas (intracranial but arising from a cranial nerve), we modified the previously published model for gliomas. In brief, *Nf2*−/− cells were implanted between the pia and arachnoid meninges in nude mice (8 weeks old) bearing transparent cranial windows [4]. In the second model, we reproduced the nerve microenvironment using the mouse sciatic nerve [4]. This environment had previously been shown to be suitable for schwannoma growth. In both models, approximately a million cells were injected with a 28.5-gauge needle to generate schwannomas.

Mouse Angiogenesis PCR Array

RNA was extracted from tumor cells with or without merlin/NF2 using RNeasy Mini Kit (Qiagen, Valencia, CA), DNase-treated (Promega, Madison, WI), and retrotranscribed by RT^2 First Strand Kit (SA Bioscience, Valencia, CA). Mouse Angiogenesis RT^2 Profiler PCR Array and RT^2 Real-time SyBR Green/ROX PCR Mix were purchased from SA Biosciences. PCR was performed on either Stratagene Mx3000P or Mx3005P (Agilent Technologies). We used the ΔC_t method for data analysis. For each gene fold, changes were calculated as difference in gene expression between cells expressing merlin/NF2 and that without. A positive value indicates gene up-regulation and a negative value indicates gene down-regulation.

DNA Microarray Analysis

Total RNA was isolated from merlin/NF2 cells (RNeasy Mini Kit; Qiagen) according to recommended Affymetrix (Santa Clara, CA) protocols. Total RNA was checked for RIN score using an Agilent 2100 Bioanalyzer with an RNA Nano 2000 chip using methods according to the Agilent Bioanalyzer manual. Samples were processed using 20 μg of starting total RNA and were amplified and labeled using the GeneChip Expression 3′-Amplification Reagents One-Cycle complementary DNA (cDNA) synthesis kit (P/N 900431 from Affymetrix) followed by the GeneChip Expression 3′-Amplification Reagents for IVT Labeling (P/N 900449 from Affymetrix). The labeled sample was then fragmented using 5× fragmentation buffer contained in the above kits and hybridized to the chip overnight in a hybridization cocktail containing Control Oligo B2, biotinylated hybridization controls, acetylated bovine serum albumin, herring sperm DNA, 2× hybridization buffer in an Affymetrix Model 640 Hybridization oven for ~16 hours at 45°C with rotation at 60 RPM. The chips were then washed using buffers A and B in a Model 450Gene Chip Fluidics station and then scanned using an Affymetrix Model 3000 GeneChip Scanner with Autoloader. Scanning and analysis were carried out using Affymetrix GCOS software. The raw data were then normalized using MAS5.0 and scaled to a factor of 500. Comparative analysis was then performed by using a two-sided *t* test with a minimum SD of 1.0. We used false discovery rate (FDR) adjustment to account for multiple testing hypothesis.

Semiquantitative PCR

Total RNA was extracted from *Nf2*−/− or HEI193 cells using the RNeasy Mini Kit (Qiagen) according to the instruction manual. Genomic DNA was digested using the RNase-free DNase I (Qiagen) to ensure the complete removal of DNA contamination. The amount of total RNA was quantified by absorbance at 260 nm (NanoDrop, Wilmington, DE). Five hundred nanograms of RNA from each sample was transcribed to cDNA using SuperScript III RNase H^- Reverse Transcriptase (Invitrogen). PCR was performed in a thermal cycler (DYAD). PCR products were then resolved in a 2% agarose gel by electrophoresis, and DNA images were captured with the UV transilluminator (Bio-Rad, Hercules, CA). Glyceraldehyde-3-phosphate dehydrogenase (*Gapdh*) gene was amplified in each PCR experiment as an internal loading control.

Determination of Rac1 Activity

Rac1 activity was measured with Rac1 (BK035) activation assay biochem kit (Cytoskeleton) according to the manufacturer's protocol. Cells were first washed with phosphate-buffered saline (PBS) and then lysed with lysis buffer supplemented with protease inhibitors. About 100 μg of lysates was precleared, and 10 μl of PAK-PBD beads was added for pull-down of activated Rac1. Positive (GTPrS) and negative (GDP) controls were included to show the functionality of the activity assay. After rocking at 4°C for 1 hour, we washed the beads once and boiled them at 100°C for 2 minutes. Protein lysates were subsequently resolved in a 8% to 16% gradient gel (Invitrogen) and transferred them to a polyvinylidene fluoride membrane, and Rac1 expression (corresponds to its activity) was detected using standard Western blot analysis. Ten nanograms of His-tagged Rac1 recombinant protein was loaded as a control.

Western Blot Analysis

Cells were rinsed with cold PBS and lysed in an appropriate volume of lysis buffer. Protein concentration was measured with bicinchoninic acid (BCA) protein assay kit (Pierce, Rockford, IL) according to the manufacturer's instructions. Appropriate volumes of protein lysates were then mixed with 4× SDS gel-loading buffer, boiled at 100°C for 5 minutes, and resolved in 8% to 16% gradient polyacrylamide gels (Invitrogen). Proteins were subsequently transferred onto polyvinylidene fluoride membrane (0.45 μm; Thermo Scientific, Rockford, IL), and the membrane was blocked with 5% nonfat milk in Tris-buffered saline with Tween 20 for 1 hour. Blots were then incubated with appropriately diluted primary and horseradish peroxidase–conjugated secondary

antibodies, each for 1 hour at room temperature. Finally, blots were developed with enhanced chemiluminescence solutions and exposed onto HyBlot CL (Denville Scientific, Metuchen, NJ).

Immunohistochemistry

Mice were perfusion fixed with 4% formaldehyde in PBS. Perfused tumors were extracted, postfixed in formaldehyde at 4°C for 4 to 5 hours, and incubated with 30% sucrose overnight at 4°C with constant rocking. Sciatic nerve tumors were then embedded in optimal cutting temperature freezing medium and frozen for sectioning. Sections (10 μm thick) were first air-dried for 30 minutes at room temperature and postfixed with acetone for 5 minutes at −20°C. Double staining was performed using CD31 (1:150, MAB 1398Z; Chemicon) and desmin (1:300, A0611; Dako, Carpinteria, CA). Detection was carried out using secondary antibodies (or streptavidin) labeled with fluorophores of different wavelength (fluorescein isothiocyanate, Cy3, and Cy5). Confocal images were acquired using a FluoView 500 confocal microscope (Olympus, Center Valley, PA). A constant surface area (0.4 mm^2) was imaged in all cases.

Blood Vessel Permeability Measurement

Changes in vessel permeability in sciatic nerve tumors was examined with Evans Blue dye extravasation assay. Mice were first anesthetized with ketamine (10 mg/kg)/xylazine (1 mg/kg) mix and then injected with 1 mg/kg 3% Evans Blue dissolved in 0.9% saline. After 20 minutes, mice were perfusion fixed with 4% formaldehyde in PBS, and sciatic nerve tumors were extracted. Tumors were weighed (wet weight), cut, and immersed in 1 ml of formamide at 56°C overnight to extract the Evans Blue dye that was extravasated out of the vessels. The following day, tissues were removed from the formamide, and the absorbance (OD_{620nm}) of the samples was measured with a spectrophotometer. Results were expressed as microgram of Evans Blue per milligram of tumor tissue based on a standard curve of Evans Blue and the wet weight of the tumor.

Quantification of Vessel Area and Perivascular Cell Coverage

Quantification of the immunohistochemistry (IHC) sections for vessel area and pericyte coverage was completed with a custom image process program written in MATLAB (MathWorks). On the basis of CD31 fluorescence intensity, images were thresholded to achieve vessel segmentation. To determine the vessel area (a surrogate for vessel density), the total CD31 area was calculated and divided by the total area of 4′,6-diamidino-2-phenylindole (DAPI)–stained nuclei. In addition, from the segmented images, the average vessel diameter was measured using automated protocols. Finally, the segmented CD31 images were dilated by 4 μm and colocalized with desmin fluorescence images to determine the amount of desmin+ cells in vessel regions (pericytes coverage).

Statistical Analysis

We used the unpaired, two-tailed Student's *t* test for comparison between two samples. One-way analysis of variance Fisher test followed by Tukey honestly significant difference test was used for multiple comparisons with a 95% confidence level. For survival rate, we plotted the survival distribution curve with the Kaplan-Meier method followed by log-rank testing (XLSTAT software, New York, NY). We considered the difference between comparisons to be significant when $P < .05$ for all the statistical analysis. All values were presented as mean ± SEM.

Results

Class 3 Semaphorin Expression Levels Are Specifically Downregulated in the Absence of Wild-type Copies of Merlin/NF2

We have previously shown that expression levels of SEMA3A and SEMA3F are significantly downregulated in both NF2-related and sporadic schwannomas [3]. To examine more systematically whether secreted class 3 SEMAs are specifically affected in tumor cells that do not express wild-type merlin/NF2, we compared the expression levels of class 3 SEMAs between primary human and mouse Schwann cells with HEI193 (human merlin-deficient Schwann cells) and *Nf2*−/− (mouse merlin-deficient Schwann cells), respectively. This comparison consistently revealed that the expression of most of SEMA3s was largely downregulated in the absence of merlin (Figure 1*A*) without affecting that of NRP or plexins (data not shown). Knocking down the expression of merlin in primary mouse Schwann cells recapitulated similar observations (Figure 1*B*). When we reintroduced merlin into mouse *Nf2*−/− schwannoma cells [the *Nf2*−/−(pWZL-NF2)], we specifically restored expression of SEMA3B and SEMA3F (Figure 1*C*). Of note, SEMA3F, in particular, is a potent antiangiogenic factor [19,21].

To determine whether other angiogenic factors in addition to SEMA3F were regulated by merlin, we compared the messenger RNA (mRNA) expression profile of 87 angiogenic factors between *Nf2*−/−(pWZL) and *Nf2*−/−(pWZL-NF2) cells with mouse angiogenesis array. We found that the expression of TSP2, a well-described antiangiogenic factor, was also prominently upregulated with merlin reintroduction. There was a 7.04 ± 1.85-fold increase ($P < .02$) of *thbs2* mRNA that encodes TSP2 protein. This increase is specific for TSP2 because there was only a slight but insignificant increase for that of *thbs1* (2.3 ± 0.78, $P = .6$, $n = 3$). Interestingly, we did not detect any significant change of VEGF or PDGFa expression, two very potent proangiogenic factors (0.9 ± 0.56- and 1.4 ± 0.36-folds, respectively). These data suggest that reintroduction of merlin/NF2 specifically tips the angiogenesis balance to antiangiogenic by increasing antiangiogenic factors rather than decreasing proangiogenic factors. We then confirmed up-regulation of TSP2 and SEMA3F at the mRNA level by DNA microarray analysis (TSP2: 7.9 ± 0.7-fold increase and SEMA3F: 15.3-fold increase). Finally, we determined that the up-regulation of SEMA3F and TSP2 was seen in the protein level (Figure 1*D*). These data indicate that merlin regulates the expression of two secreted antiangiogenic factors (SEMA3F and TSP2) that could potentially modify the tumor microenvironment of schwannomas.

Merlin/NF2 Regulates Expression of SEMA3F and TSP2 through a Rac1-Dependent Pathway

To investigate the mechanism(s) whereby merlin/NF2 regulates expression of SEMA3F and TSP2, we used protein inhibitors and retroviral RNA interference in our schwannoma cells. One likely candidate modulating this pathway could be Rho GTPase because 1) Rac1 [26] and cdc42 [27] activity and intracellular localization were altered in human schwannoma cells deficient in merlin expression, 2) Rac1 was found to be able to regulate the expression of TSP2 in endothelial cells [28], and (3) RhoA and Rho-associated coiled-coil forming protein serine/threonine kinase (ROCK) were found to mediate the collapsing activity of SEMA3F [21]. Thus, in our system, we examined Rac1 activity. Compared with the cells that were reintroduced with wild-type merlin, we found that Rac1 activity is indeed increased in the merlin-deficient counterpart (Figure 2*A*). Next, we treated *Nf2*−/

–(pWZL-NF2) cells with exoenzyme C3 transferase (an ADP ribosyl transferase that selectively ribosylates RhoA, RhoB, and RhoC proteins on asparagine residue 41, rendering them inactive), Y-27632 (a specific inhibitor of the ROCK family of protein kinases), or a Rac1 inhibitor to examine which member in the Rho family GTPase is responsible for the induction of SEMA3F and TSP2 on the reintroduction of merlin/NF2. We found that Rac1 inhibition itself was enough to almost completely abrogate the induction of SEMA3F and TSP2 (Figure 2*B* and quantified in Figure 2*C*). Blocking RhoA/B/C or ROCK did not produce any significant and detectable suppression of either SEMA3F or TSP2.

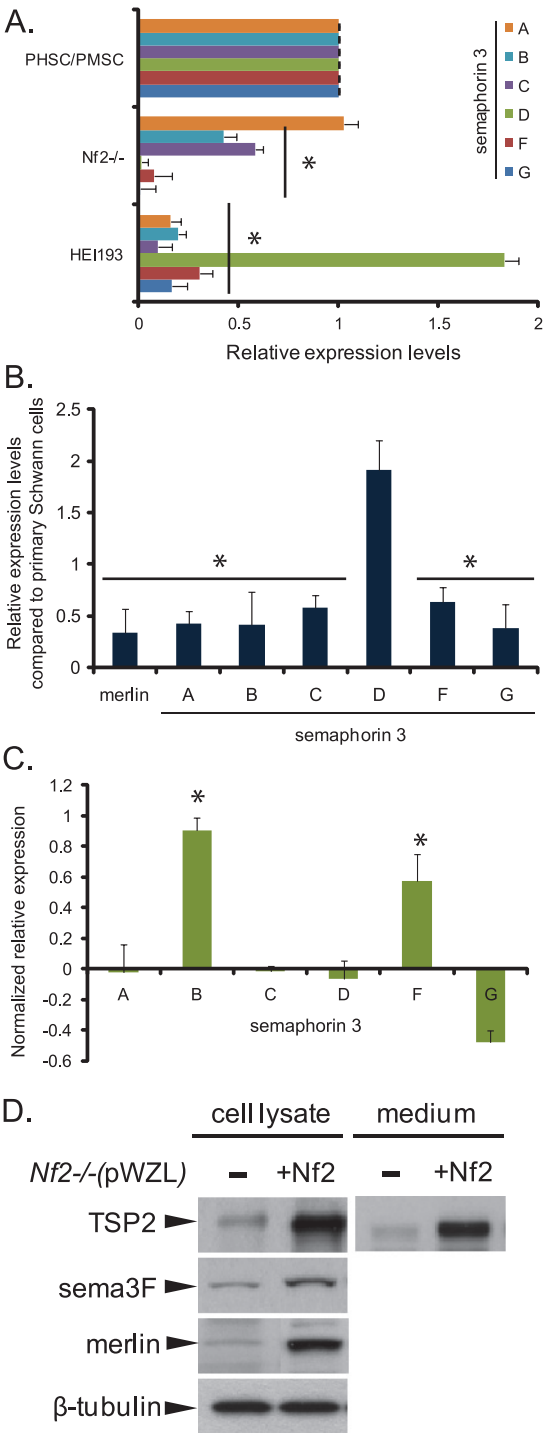

To further confirm that Rac1 is the specific member in the Rho GTPase family regulating SEMA3F and TSP2 expression, we knocked down the expression of Rac1 genetically in the *Nf2*–/–(pWZL-NF2) cells by Rac1 shRNA retroviruses achieving a 60% reduction of Rac1 expression (Figure 2*D*). This knockdown resulted in a marked suppression of SEMA3F and TSP2 production, similar to the data that we obtained with Rac1 inhibitors. To investigate the consequence of this genetic modification, we treated endothelial tubes formed by HUVECs with conditioned medium collected from *Nf2*–/–(NF2 + Rac1 – scramble) or *Nf2*–/–(NF2 + Rac1 – shRNA). In endothelial tubes treated with the Rac1 shRNA conditioned medium, we observed a significant maintenance of tube structure compared with endothelial tubes treated with scramble conditioned medium where we found tube collapse (Figure 2*D*, 5.3 ± 0.47 more tubes in HUVECs treated with the Rac1 shRNA conditioned medium compared with the scrambled control). These data suggest that an increase in Rac1 activity in the absence of merlin leads to a subsequent decrease in SEMA3F and TSP2, thereby reducing the antiangiogenic effects of schwannoma cells.

SEMA3F Normalizes Nf2–/– *Tumor Vessels Resulting in Reduced Tumor Size and Improvement of Overall Survival*

To determine whether this merlin-mediated regulation of SEMA3F and TSP2 observed *in vitro* has a functional role in schwannoma angiogenesis and tumor progression *in vivo*, we generated *Nf2*–/– cell lines that constitutively express high levels of either SEMA3F or TSP2 compared with control cells (Figure 3*A*). We also confirmed that these cell lines continued to express SEMA3F or TSP2 in an orthotopic model of brain tumor (Figure 3*B*). Finally, to further confirm that the secreted SEMA3F is biologically active in these cells, we used a cytoskeleton

Figure 1. Merlin regulates expression of class 3 semaphorins and TSP2. (A) Merlin-deficient tumor cells have significantly lower SEMA3 expression compared to their primary counterparts. Semiquantitative PCR was done to examine the expression profile of SEMA3s in primary human Schwann cells (PHSC), primary mouse Schwann cells (PMSC), mouse schwannoma cells (*Nf2*−/−), and human schwannoma cells (HEI193). Expression levels of SEMA3s in primary cells were normalized with an input control (gapdh), and that of tumor cells was compared accordingly and expressed as relative expression levels. $n = 3$ and $^*P < .01$. (B) Merlin expression positively correlates with SEMAs in primary Schwann cells. Merlin expression was downregulated with lentiviral particles expressing merlin shRNA. Total RNA was then extracted and reverse transcribed, and the expression of merlin and SEMA3s was examined with semiquantitative PCR. Scramble-infected primary Schwann cells were used as a control for comparison (set to 1). $n = 3$ and $^*P < .01$ compared with the expression in scramble control. (C) Reintroduction of wild-type merlin restores expression of SEMA3B and SEMA3F. Wild-type merlin (pWZL-NF2) was reintroduced into *Nf2*−/− cells with retroviruses. Infected cells were selected with hygromycin B at 200 μg/ml for several weeks, and single clones were selected. Expression of SEMAs in pWZL-NF2 was compared with a control schwannoma cell line that was infected with an empty vector pWZL. $n = 3$ and $^*P < .01$. (D) Reintroduction of merlin upregulates SEMA3F and TSP2 protein expression in schwannoma cells. Protein lysates and conditioned medium from *Nf2*−/−(pWZL) and *Nf2*−/−(pWZL-NF2) were resolved in a gradient gel and expression of SEMA3F, and TSP2 was examined by Western blot analysis. Merlin blot confirmed the successful reintroduction, and β-tubulin was used as an input control. $n = 3$.

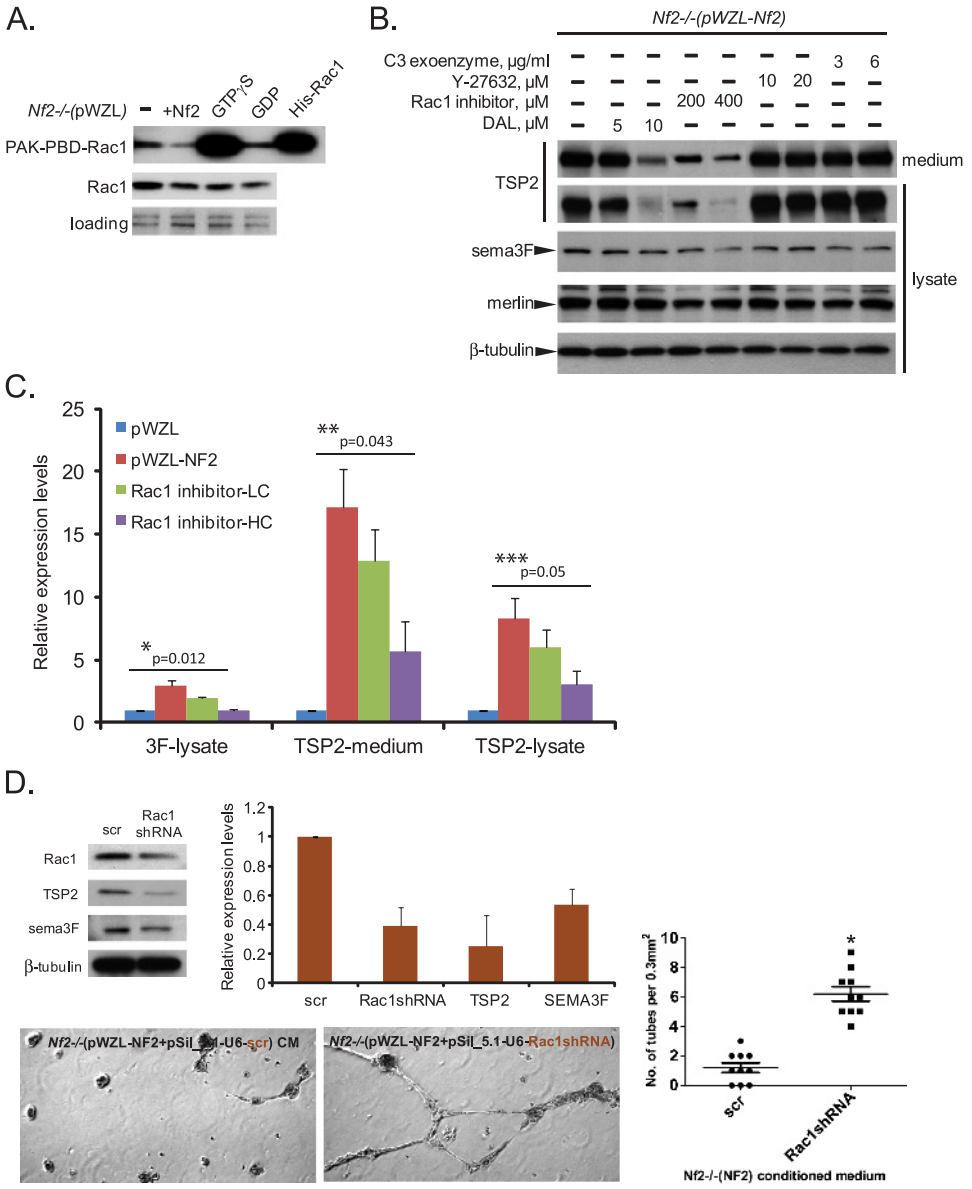

Figure 2. Merlin regulates expression of SEMA3F and TSP2 through a Rac1-dependent pathway. (A) Rac1 activity and expression increases in schwannoma cells that are deficient in merlin. PAK-PBD-Rac1 indicates active Rac1, and Rac1 represents the total form. PAK indicates p21 activated kinase 1; PBD, p21 binding domain. (B) Inhibiting Rac1 activity diminishes the expression of SEMA3F and TSP2 induced by merlin. Rho GTPases (cdc42, Rac1, and ROCK) were inhibited with specific inhibitors at increasing concentrations. One day after incubation, both medium and lysates were collected, and the expression levels of SEMA3F and TSP2 as well as merlin were analyzed with Western blots. (C) Quantification of SEMA3F and TSP2 expression levels in Rac1-inhibited conditions. Expression levels of SEMA3F and TSP2 were measured and normalized with β-tubulin. The normalized values in the control line (pWZL) were then set to 1, and the expression levels of SEMA3F and TSP2 in other conditions were compared with the control accordingly. HC indicates high concentration; LC, low concentration. $n = 3$ independent Western blots. *$P = .012$. **$P = .043$. ***$P = .05$. (D) Suppressing Rac1 expression by RNA interference specifically reduces SEMA3F and TSP2 expression and results in a more intact network of endothelial tubes. Rac1 shRNA (or scramble [scr]) was transduced into *Nf2*−/−(pWZL-NF2) cells by retroviruses, and the infected cells were selected by puromycin at 1 μg/ml for 3 days. Conditioned medium from scr (i) or Rac1 shRNA (ii) was then added to the endothelial network formed by HUVECs. Phase-contrast images were captured 36 hours after the addition of conditioned medium to examine the biologic effect of Rac1 knockdown. The tube formation per field was calculated to be 5.3 ± 0.47 times higher in Rac1 knockdown conditioned medium wells compared with control conditioned medium.

collapse assay that directly shows the activity of SEMA3F [21]. In cells treated with conditioned medium produced from *Nf2*−/−(SEMA3F), almost 90% of U87MG cells collapsed within 5 hours, whereas cells treated with control *Nf2*−/−(dsred) conditioned medium remained unchanged (Figure 3*C*). We also found that conditioned medium obtained from *Nf2*−/−(TSP2) decreased proliferation of HMVECs by more than 50% in 4 days after treatment compared with that produced from *Nf2*−/−(dsred) (Figure 3*D*).

Given a functional role of SEMA3F and TSP2 in our cell lines, we implanted *Nf2*−/−(SEMA3F), *Nf2*−/−(TSP2), or *Nf2*−/−(dsred) into

the sciatic nerve of nude mice and examined the effect of these molecules on the progression of schwannoma. We found that nerve tumors with ectopic SEMA3F expression were much smaller compared with dsred control tumors (Figure 4*A*). Nevertheless, we were unable to observe any prominent antitumor effect of TSP2 in the development of these tumors (data not shown). When we analyzed the tumor vessels in these tumors by immunohistochemistry, we found that overexpression of SEMA3F reduced total number of $CD31^+$ vessels per area, a surrogate for vessel density, by 25% without affecting the diameter of the vessels (Figure 4*B*), whereas TSP2 did not affect vessel density or diameter. Moreover, SEMA3F was able to restore pericyte coverage on tumor vessels—we measured a 2.5-fold increase in pericyte coverage based on desmin staining (Figure 4*C*). Accompanying the increase of pericyte coverage, there was a 30% reduction of permeability in sciatic nerve tumors with SEMA3F overexpression (Figure 4*D*). When we implanted tumors using another orthotopic model of NF2 in the brain, *Nf2*−/−(SEMA3F) brain tumors also grew more slowly and were smaller in size, and the mice bearing these brain tumors had a significantly better overall survival rate (Figure 4*E*; dsred, 17.9 ± 1.5 days; SEMA3F, 26.5 ± 1.3 days; $P < .01$). However, consistent with the lack of effects in the nerve tumor, *Nf2*−/−(TSP2) tumor-bearing mice had no improvement in survival over control tumor-bearing mice. Taken together, although reintroduction of merlin upregulates both SEMA3F and TSP2- in schwannoma microenvironment, increased expression of TSP2 merely does not result in any observable angiogenic changes. It is more likely that merlin-SEMA3F signaling keeps the angiogenic balance in check. The role of TSP2 in Schwann cells or the schwannoma microenvironment remains to be further investigated.

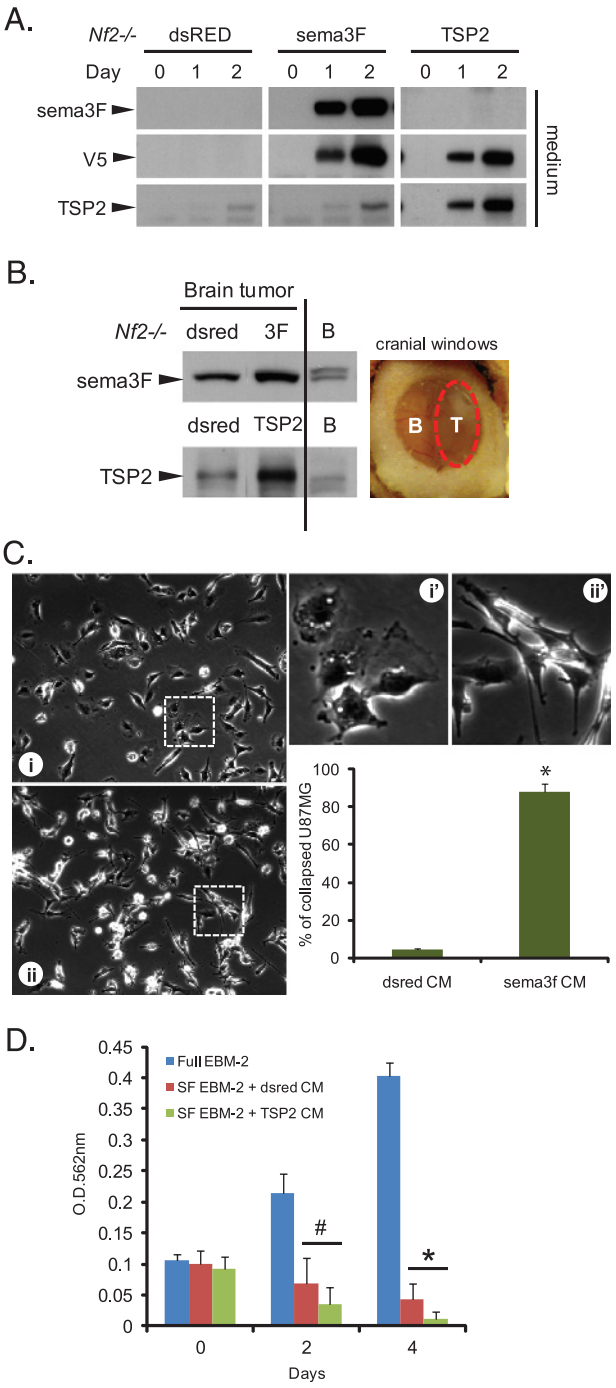

Figure 3. Characterization of expression and function of SEMA3F and TSP2 in genetically modified schwannoma cells. (A) Schwannoma cells that are reintroduced with SEMA3F or TSP2 secrete these proteins in a time-dependent manner. *Nf2*−/− cells were infected with retroviral particles expressing either pMOWSdSV-SEMA3F or -TSP2. Almost 100% of the cells were positive for the reintroduction after two overnight infections, as evident by the red fluorescence from the dsred control. Conditioned medium (free of serum) was collected from each cell line, and 20 μl of medium was resolved in a gradient gel for the detection of SEMA3F and TSP2. V5 blots were used to confirm the expression of exogenously introduced protein. (B) Schwannoma cells continue to express high levels of SEMA3F or TSP2 in the brain environment. Schwannoma cells expressing either SEMA3F or TSP2 were implanted into the brain parenchyma, and tumors were allowed to form. Tumors were extracted when reached 10 × 10 mm in size, and protein lysates were used for the detection of SEMA3F or TSP2. B indicates brain; T, tumor. (C) Conditioned medium collected from SEMA3F expressing schwannoma cells is able to collapse U87MG cells. *Nf2*−/−(SEMA3F) conditioned medium was added to U87MG cells at a 1:10 dilution (ii and ii′) and *Nf2*−/−(dsred) conditioned medium was used as a control (i and i′). Phase contrast images were captured 5 hours after the addition of SEMA3F conditioned medium and the number of collapsed cells were counted and presented graphically in lower panel. To define a cell that was collapsed, it had to possess a shrunken cell body and multiple extended processes (ii′). Controls cells were normally flat without many processes (i′). CM indicates conditioned medium. $n = 3$. $^*P < .01$. (D) Conditioned medium collected from TSP2 expressing schwannoma cells inhibits proliferation of HMVECs. Schwannoma cells were lysed with the same volume of protein lysis buffer, and 5 μl of precleared lysate was quantified by BCA assay. The total amount of cells in each condition was represented as the absorbance at 562 nm. SF indicates serum-free medium. $n = 3$. $^*P < .01$. $^{\#}$Not significant.

Discussion

Schwannomas typically progress slowly and are not considered to be angiogenic tumors. However, our recent review of surgical archival specimen revealed a proangiogenic profile defined by number and size of vessels combined with quantification of VEGF expression and SEMA3F loss [3]. Furthermore, in a recent preclinical study, we showed that loss of the *Nf2* gene was accompanied by the loss of SEMA3F and that treatment with anti-VEGF therapies resulted in sustained decreases in growth rate and vessel permeability [4]. These

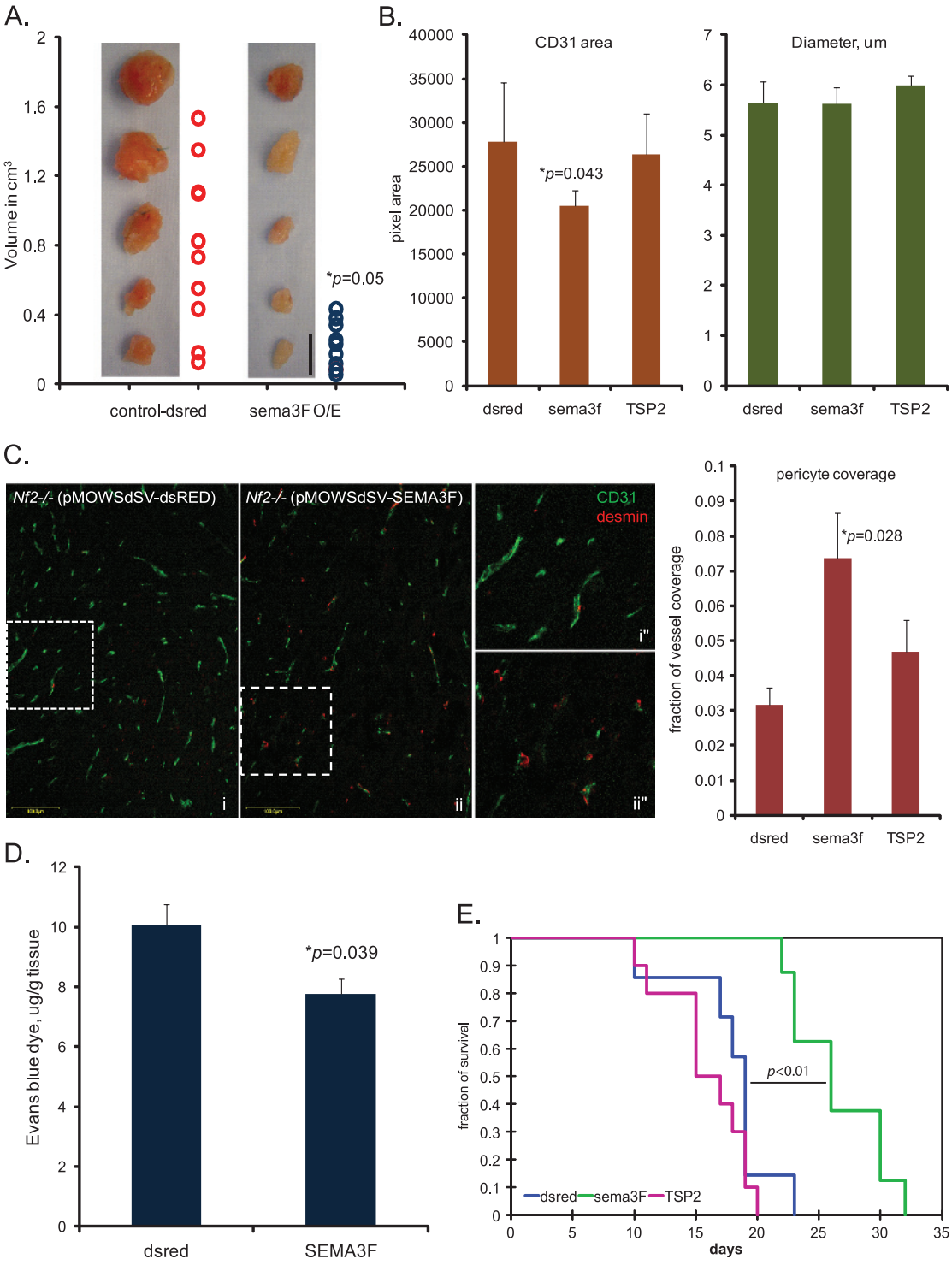

Figure 4. SEMA3F normalizes schwannoma vessels and reduces tumor burden. (A) SEMA3F reexpression reduces sciatic nerve tumor burden. Animals were perfusion fixed, and tumors were extracted approximately 2 weeks after implantation. Tumor volume was measured and compared accordingly. Scale bar, 1 cm. O/E indicates overexpression. $n = 10$. *$P = .05$. (B) SEMA3F reexpression reduces $CD31^+$ area without affecting the vessel diameter. Frozen sections of sciatic nerve tumor generated from each schwannoma line as indicated in the diagram were immunostained with anti-CD31 to reveal tumor vessels. Overexpression of SEMA3F reduced vascularity by 25% compared with the dsred control, without influencing the blood vessel diameter. $n = 7$. *$P = .043$. (C) SEMA3F reexpression markedly increases pericyte coverage. Frozen sections of sciatic nerve tumor generated from *Nf2*−/−(dsred) (i and i″) and *Nf2*−/−(SEMA3F) (ii and ii″) were costained with anti-CD31 and anti-desmin. The overlapping of desmin and CD31 area was quantified to indicate pericyte coverage. Scale bar, 100 μm. $n = 7$. *$P = .028$. (D) SEMA3F reexpression reduces tumor vessel permeability. Evans Blue dye extravasation assay was used to examine vessel permeability. Amount of Evans Blue dye in tumor tissues was expressed as micrograms of dye per gram of tissue. $n = 3$. *$P = .039$. (E) SEMA3F extends overall survival in mice bearing brain tumors. SEMA3F reexpression extends overall survival in mice bearing brain tumors, whereas TSP2 does not show any beneficial effect. $n = 7$ for dsred, $n = 8$ for SEMA3F, and $n = 10$ for TSP2. *$P < .01$ by log-rank test.

findings led us to propose that the loss of merlin could contribute to an abnormal tumor vasculature by disrupting the delicate balance of proangiogenic and antiangiogenic factors.

In the current study, we indeed found that merlin regulates expression of class 3 SEMAs through the Rho GTPase Rac1 specifically, but not the other close family members such as cdc42 or Rho A. Rac1 expression levels were found upregulated as well as Rac1 protein translocated to the membrane ruffles in human schwannoma cells lacking wild-type copies of merlin [26]. Merlin was subsequently found to regulate cell proliferation and contact inhibition dominantly by interfering with the guanine exchange of Ras and Rac and its downstream signaling cascades involving Raf and ERK [29]. In addition, Rac1 activity has been reported to modulate growth cone collapse induced by SEMA3A [30–32]. Our findings established a signaling cascade connection whereby Rac1 works downstream of merlin and upstream of SEMA3F (Figure 5). However, as blocking the expression and activity of Rac1 was able to virtually erase SEMA3F expression, it is likely that the regulation involves multiple steps. Histone deacetylase may represent an intermediate step between Rac1 and SEMA3F because its activity directly correlated with active Rac1 [33,34] and histone deacetylase inhibition markedly stimulated the activity of SEMA3F [35].

By reintroducing SEMA3F into merlin-deficient schwannoma cells, we further confirmed the role of SEMA3F as an antiangiogenic factor in our experimental settings. Our data are consistent with the published data that expression of SEMA3F was specifically downregulated in NF2-driven schwannomas [3] as well as in tumors of the pancreatic and cervical origins [36] and that reexpressing SEMA3F is able to decrease tumor vascularity and restore pericyte coverage *in vivo* [19,36]. On the basis of this potent angioinhibitory effect, we are the first to show that orthotopic schwannoma tumors overexpressing SEMA3F were smaller in size and the lower tumor burden resulted in extension of overall survival, similar to the effect observed in mice carrying pancreatic tumors overexpressing SEMA3A [36]. Furthermore, we showed that reexpressing SEMA3F contributed to an effective decrease in permeability. Although much less is known about the blood-nerve barrier, permeability has been shown to play a role in schwannomas and its control might have a direct benefit [3,4].

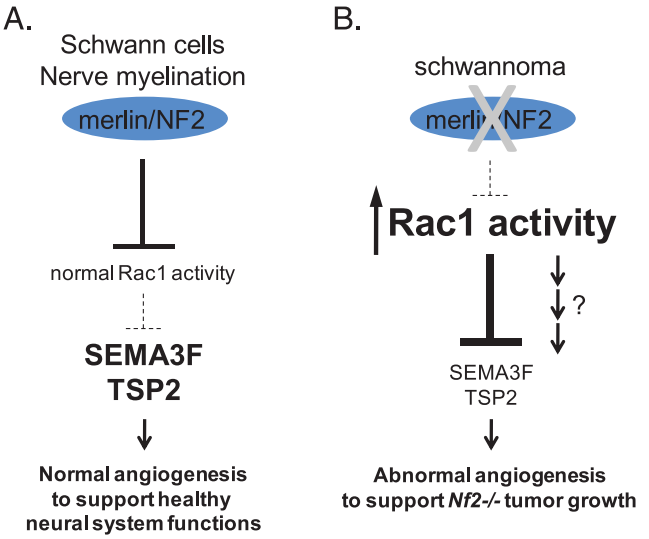

Figure 5. The proposed mechanism by which merlin loss supports neurofibromatosis angiogenesis. In the presence of wild-type merlin, Rac1 activity is maintained at a normal state, as well as the levels of SEMA3F/TSP2. The physiological balance of proangiogenic and antiangiogenic factors supports normal vascularity that is necessary for healthy neural system functions (A). However, in Schwann cells that are deficient in merlin, the increased Rac1 activity leads to an enhanced suppression of SEMA3F/TSP2 expression—the augmented relative VEGF levels and the subsequent pathologic changes thus are able to drive abnormal angiogenesis to further support the nutritious need for the unlimited proliferation of schwannoma cells (B). It is likely that the mechanism(s) by which Rac1 suppresses SEMA3F and TSP2 involves multiple steps, and the precise regulatory mechanisms remain to be investigated.

In addition to SEMA3F, we also found that TSP2 was highly upregulated in *Nf2*−/− schwannoma cells that were reintroduced with wild-type merlin. This up-regulation is consistent with the idea that Rac1 is working upstream because it has been reported that a constitutively active mutant of Rac1 (RacV12) is able to regulate TSP2 expression at the transcription level in endothelial cells [28]. However, we did not observe any detectable antiangiogenic properties with merlin-deficient schwannoma cells that overexpress TSP2 *in vivo* (Figure 4). In general, thrombospondins are antiangiogenic [37]. However, because TSP1 and TSP2 are composed of multiple functional domains and each has its own receptors, the consequence of TSP expression may not always be simply antiangiogenic. In fact, there is ample evidence that TSP1 is not antiangiogenic and even proangiogenic [38–41]. In all these studies, it can be concluded that the overall angiogenic outcome initiated by TSPs is largely determined by 1) specific domain interaction with appropriate receptors, (2) absolute concentration of TSPs, and/or (3) the unique microenvironment of the experimental models. Because TSP2 has an equivalent domain structure to TSP1 and the microenvironment of nerve tumors is not completely explored, it is plausible to assume that the domain/receptor interactions between the tumor-secreted TSP2 and the stroma could be complex, and thus, the overall angiogenic outcome is difficult to predict. Moreover, because TSP2 has pleiotropic effects and is involved in processes as disparate as bone growth, homeostasis, and foreign body response [42], it is also possible that TSP2 is not simply angioinhibitory in the nerve microenvironment. Nevertheless, it is essential to establish a causal correlation between TSP2 and merlin in clinical samples of NF2-related schwannomas so that the precise role of TSP2 can be investigated in the pathogenesis of schwannomas.

Furthermore, there are few data on the regulation and interaction between SEMA3F, RAC1, and TSP2. Our data suggest SEMA3F is upstream of TSP2 because TSP2 is increased with SEMA3F expression, but the reverse is not true. SEMA3F works upstream of RhoA and ROCK because this signaling cascade leads to the activation of cofilin and actin depolymerization in both glioma and endothelial cells [21]. In addition, RhoA and ROCK are able to suppress TSP1 through Myc, a close member of TSP2 [43]. Interestingly, Myb, a nuclear transcription factor in the same class of Myc, has been shown to suppress TSP2 specifically [44]. Therefore, we speculate that SEMA3F works upstream of TSP2, possibly through RhoA, ROCK, and Myb.

In summary, this study revealed that merlin/NF2, a tumor suppressor gene, on top of its antiproliferative function on contact inhibition, also influenced tumor angiogenesis by regulating expression of SEMA3F, a potent angioinhibitory factor, and this regulation worked through Rac1. This study further advanced our knowledge that angiogenesis is essential in benign tumor progression, and by modulating the relative balance of proangiogenic and antiangiogenic components

in these tumors, one can successfully control tumor development. This study provides a mechanism for the potential "angiogenic switch" in NF2-driven schwannoma. Benign tumors such as schwannomas progress very slowly, and understanding the mechanism behind the modulation of the proangiogenic and antiangiogenic balance will contribute to improving treatment of these tumors. Although treatment with anti-VEGF therapies has proven successful so far, the long-term treatment of these patients necessitates the identification of new therapeutic regimens. To date, although SEMA3F is well established as an inhibitor of angiogenesis, the regulatory mechanisms of SEMA3F, or other secreted SEMAs that possess potent antiangiogenic properties, are not completely understood. In fact, small molecules that can stimulate SEMA3s expression or activity have not been developed. We strongly believe that more effort should be focused on finding drugs/small molecules that can enhance the SEMA-NRP-plexin signaling event. Modulating angiogenic balance by inhibiting proangiogenesis (blocking VEGF [4]), or promoting antiangiogenesis (reintroducing SEMA3s, this study), proved to be a successful way to control schwannoma progression and should be considered as a novel approach to treat neurofibromatosis-related tumors similar to malignant tumors [9].

Acknowledgments

The authors thank Sylvie Roberge and Carolyn Smith for their technical expertise, Padera T. Timothy and Lei Xu for discussions and guidance, and Andrew B. Gladden, Andrea I. McClatchey, and Brian Seed (Massachusetts General Hospital and Harvard Medical School, Boston, MA) for providing critical reagents.

References

[1] Asthagiri AR, Parry DM, Butman JA, Kim HJ, Tsilou ET, Zhuang Z, and Lonser RR (2009). Neurofibromatosis type 2. *Lancet* **373**, 1974–1986.

[2] Mrugala MM, Batchelor TT, and Plotkin SR (2005). Peripheral and cranial nerve sheath tumors. *Curr Opin Neurol* **18**, 604–610.

[3] Plotkin SR, Stemmer-Rachamimov AO, Barker FG II, Halpin C, Padera TP, Tyrrell A, Sorensen AG, Jain RK, and di Tomaso E (2009). Hearing improvement after bevacizumab in patients with neurofibromatosis type 2. *N Engl J Med* **361**, 358–367.

[4] Wong HK, Lahdenranta J, Kamoun WS, Chan AW, McClatchey AI, Plotkin SR, Jain RK, and di Tomaso E (2010). Anti–vascular endothelial growth factor therapies as a novel therapeutic approach to treating neurofibromatosis-related tumors. *Cancer Res* **70**, 3483–3493.

[5] Caye-Thomasen P, Baandrup L, Jacobsen GK, Thomsen J, and Stangerup SE (2003). Immunohistochemical demonstration of vascular endothelial growth factor in vestibular schwannomas correlates to tumor growth rate. *Laryngoscope* **113**, 2129–2134.

[6] Caye-Thomasen P, Werther K, Nalla A, Bog-Hansen TC, Nielsen HJ, Stangerup SE, and Thomsen J (2005). VEGF and VEGF receptor-1 concentration in vestibular schwannoma homogenates correlates to tumor growth rate. *Otol Neurotol* **26**, 98–101.

[7] Koutsimpelas D, Stripf T, Heinrich UR, Mann WJ, and Brieger J (2007). Expression of vascular endothelial growth factor and basic fibroblast growth factor in sporadic vestibular schwannomas correlates to growth characteristics. *Otol Neurotol* **28**, 1094–1099.

[8] Uesaka T, Shono T, Suzuki SO, Nakamizo A, Niiro H, Mizoguchi M, Iwaki T, and Sasaki T (2007). Expression of VEGF and its receptor genes in intracranial schwannomas. *J Neurooncol* **83**, 259–266.

[9] Jain RK (2005). Normalization of tumor vasculature: an emerging concept in antiangiogenic therapy. *Science* **307**, 58–62.

[10] Yazdani U and Terman JR (2006). The semaphorins. *Genome Biol* **7**, 211.

[11] Chen H, He Z, and Tessier-Lavigne M (1998). Axon guidance mechanisms: semaphorins as simultaneous repellents and anti-repellents. *Nat Neurosci* **1**, 436–439.

[12] Luo Y, Raible D, and Raper JA (1993). Collapsin: a protein in brain that induces the collapse and paralysis of neuronal growth cones. *Cell* **75**, 217–227.

[13] Puschel AW, Adams RH, and Betz H (1995). Murine semaphorin D/collapsin is a member of a diverse gene family and creates domains inhibitory for axonal extension. *Neuron* **14**, 941–948.

[14] Miao HQ, Soker S, Feiner L, Alonso JL, Raper JA, and Klagsbrun M (1999). Neuropilin-1 mediates collapsin-1/semaphorin III inhibition of endothelial cell motility: functional competition of collapsin-1 and vascular endothelial growth factor-165. *J Cell Biol* **146**, 233–242.

[15] Kessler O, Shraga-Heled N, Lange T, Gutmann-Raviv N, Sabo E, Baruch L, Machluf M, and Neufeld G (2004). Semaphorin-3F is an inhibitor of tumor angiogenesis. *Cancer Res* **64**, 1008–1015.

[16] Neufeld G, Lange T, Varshavsky A, and Kessler O (2007). Semaphorin signaling in vascular and tumor biology. *Adv Exp Med Biol* **600**, 118–131.

[17] Bielenberg DR and Klagsbrun M (2007). Targeting endothelial and tumor cells with semaphorins. *Cancer Metastasis Rev* **26**, 421–431.

[18] Takahashi T and Strittmatter SM (2001). Plexina1 autoinhibition by the plexin sema domain. *Neuron* **29**, 429–439.

[19] Bielenberg DR, Hida Y, Shimizu A, Kaipainen A, Kreuter M, Kim CC, and Klagsbrun M (2004). Semaphorin 3F, a chemorepulsant for endothelial cells, induces a poorly vascularized, encapsulated, nonmetastatic tumor phenotype. *J Clin Invest* **114**, 1260–1271.

[20] Coma S, Amin DN, Shimizu A, Lasorella A, Iavarone A, and Klagsbrun M (2010). Id2 promotes tumor cell migration and invasion through transcriptional repression of semaphorin 3F. *Cancer Res* **70**, 3823–3832.

[21] Shimizu A, Mammoto A, Italiano JE Jr, Pravda E, Dudley AC, Ingber DE, and Klagsbrun M (2008). ABL2/ARG tyrosine kinase mediates SEMA3F-induced RhoA inactivation and cytoskeleton collapse in human glioma cells. *J Biol Chem* **283**, 27230–27238.

[22] Ketteler R, Glaser S, Sandra O, Martens UM, and Klingmuller U (2002). Enhanced transgene expression in primitive hematopoietic progenitor cells and embryonic stem cells efficiently transduced by optimized retroviral hybrid vectors. *Gene Ther* **9**, 477–487.

[23] Gualdoni S, Albertinazzi C, Corbetta S, Valtorta F, and de Curtis I (2007). Normal levels of Rac1 are important for dendritic but not axonal development in hippocampal neurons. *Biol Cell* **99**, 455–464.

[24] Hung G, Li X, Faudoa R, Xeu Z, Kluwe L, Rhim JS, Slattery W, and Lim D (2002). Establishment and characterization of a schwannoma cell line from a patient with neurofibromatosis 2. *Int J Oncol* **20**, 475–482.

[25] Prabhakar S, Messerli SM, Stemmer-Rachamimov AO, Liu TC, Rabkin S, Martuza R, and Breakefield XO (2007). Treatment of implantable NF2 schwannoma tumor models with oncolytic herpes simplex virus G47Δ. *Cancer Gene Ther* **14**, 460–467.

[26] Kaempchen K, Mielke K, Utermark T, Langmesser S, and Hanemann CO (2003). Upregulation of the Rac1/JNK signaling pathway in primary human schwannoma cells. *Hum Mol Genet* **12**, 1211–1221.

[27] Flaiz C, Kaempchen K, Matthies C, and Hanemann CO (2007). Actin-rich protrusions and nonlocalized GTPase activation in Merlin-deficient schwannomas. *J Neuropathol Exp Neurol* **66**, 608–616.

[28] Lopes N, Gregg D, Vasudevan S, Hassanain H, Goldschmidt-Clermont P, and Kovacic H (2003). Thrombospondin 2 regulates cell proliferation induced by Rac1 redox-dependent signaling. *Mol Cell Biol* **23**, 5401–5408.

[29] Morrison H, Sperka T, Manent J, Giovannini M, Ponta H, and Herrlich P (2007). Merlin/neurofibromatosis type 2 suppresses growth by inhibiting the activation of Ras and Rac. *Cancer Res* **67**, 520–527.

[30] Jin Z and Strittmatter SM (1997). Rac1 mediates collapsin-1–induced growth cone collapse. *J Neurosci* **17**, 6256–6263.

[31] Kuhn TB, Brown MD, Wilcox CL, Raper JA, and Bamburg JR (1999). Myelin and collapsin-1 induce motor neuron growth cone collapse through different pathways: inhibition of collapse by opposing mutants of rac1. *J Neurosci* **19**, 1965–1975.

[32] Vastrik I, Eickholt BJ, Walsh FS, Ridley A, and Doherty P (1999). Sema3A-induced growth-cone collapse is mediated by Rac1 amino acids 17-32. *Curr Biol* **9**, 991–998.

[33] Kim YB, Yu J, Lee SY, Lee MS, Ko SG, Ye SK, Jong HS, Kim TY, Bang YJ, and Lee JW (2005). Cell adhesion status–dependent histone acetylation is regulated through intracellular contractility–related signaling activities. *J Biol Chem* **280**, 28357–28364.

[34] Gao YS, Hubbert CC, Lu J, Lee YS, Lee JY, and Yao TP (2007). Histone deacetylase 6 regulates growth factor–induced actin remodeling and endocytosis. *Mol Cell Biol* **27**, 8637–8647.

[35] Kusy S, Potiron V, Zeng C, Franklin W, Brambilla E, Minna J, Drabkin HA, and Roche J (2005). Promoter characterization of semaphorin *SEMA3F*, a tumor suppressor gene. *Biochim Biophys Acta* **1730**, 66–76.

[36] Maione F, Molla F, Meda C, Latini R, Zentilin L, Giacca M, Seano G, Serini G, Bussolino F, and Giraudo E (2009). Semaphorin 3A is an endogenous angiogenesis inhibitor that blocks tumor growth and normalizes tumor vasculature in transgenic mouse models. *J Clin Invest* **119**, 3356–3372.

[37] Bornstein P (2009). Thrombospondins function as regulators of angiogenesis. *J Cell Commun Signal* **3**, 189–200.

[38] Chandrasekaran L, He CZ, Al-Barazi H, Krutzsch HC, Iruela-Arispe ML, and Roberts DD (2000). Cell contact–dependent activation of $\alpha_3\beta_1$ integrin modulates endothelial cell responses to thrombospondin-1. *Mol Biol Cell* **11**, 2885–2900.

[39] Qian X, Wang TN, Rothman VL, Nicosia RF, and Tuszynski GP (1997). Thrombospondin-1 modulates angiogenesis *in vitro* by up-regulation of matrix metalloproteinase-9 in endothelial cells. *Exp Cell Res* **235**, 403–412.

[40] Staniszewska I, Zaveri S, Del Valle L, Oliva I, Rothman VL, Croul SE, Roberts DD, Mosher DF, Tuszynski GP, and Marcinkiewicz C (2007). Interaction of $\alpha_9\beta_1$ integrin with thrombospondin-1 promotes angiogenesis. *Circ Res* **100**, 1308–1316.

[41] Taraboletti G, Morbidelli L, Donnini S, Parenti A, Granger HJ, Giavazzi R, and Ziche M (2000). The heparin binding 25 kDa fragment of thrombospondin-1 promotes angiogenesis and modulates gelatinase and TIMP-2 production in endothelial cells. *FASEB J* **14**, 1674–1676.

[42] Bornstein P, Armstrong LC, Hankenson KD, Kyriakides TR, and Yang Z (2000). Thrombospondin 2, a matricellular protein with diverse functions. *Matrix Biol* **19**, 557–568.

[43] Watnick RS, Cheng YN, Rangarajan A, Ince TA, and Weinberg RA (2003). Ras modulates Myc activity to repress thrombospondin-1 expression and increase tumor angiogenesis. *Cancer Cell* **3**, 219–231.

[44] Bein K, Ware JA, and Simons M (1998). Myb-dependent regulation of thrombospondin 2 expression. Role of mRNA stability. *J Biol Chem* **273**, 21423–21429.